Introduction

The two-way wave equation which lies at the heart of wave-equation inversion propagates a given source wavelet through a computational mesh to forward model the seismic response for a given subsurface medium. This applies a non-linear transformation which maps the array of subsurface medium properties onto the array of predictions for surface recorded seismic measurements.

Gradient-descent optimisations can then be formulated where the deviation of the forward modelled traces **p** and the corresponding recorded traces **d** is measured by a cost function *f* to iteratively update an existing velocity model. Here we consider the adaptive and the least-squares forms of waveform inversion cost function optimisations referred to as AWI (Warner and Guasch, 2016) and FWI (Tarantola, 1988).

The key difference in the AWI and the FWI model updates occurs at the backpropagation stage of the model gradient computation and in particular with the form of the adjoint source which is backpropagated. For the AWI cost function, the expression is as follows:

$$\delta\mathbf{s} = \mathbf{D}\left(\mathbf{D}^{\mathrm{T}}\mathbf{D}\right)^{-1}\left[\frac{\mathbf{T}^{\mathbf{2}} - 2f\mathbf{I}}{\mathbf{w}^{\mathbf{T}}\mathbf{w}}\right]\mathbf{w}$$

where $\mathbf{w} = \left(\mathbf{D}^{\mathrm{T}}\mathbf{D}\right)^{-1}\mathbf{D}^{\mathrm{T}}\mathbf{p}$ i.e. the filter which transforms observed data into predicted data and *f* is the AWI cost function i.e. the norm of **w** weighted by diagonal matrix **T** divided by the unweighted norm of **w**. This contrasts with conventional FWI where instead $\delta\mathbf{s} = \mathbf{p} - \mathbf{d}$ and $f = \frac{1}{2}(\mathbf{p} - \mathbf{d})^{\mathrm{T}}(\mathbf{p} - \mathbf{d})$ i.e. simply the norm of the residual.

In AWI, the missing reflections in the model predicted data contribute to large lags and these have a greater effect on the cost function value than with FWI. This increased sensitivity to reflections and reflection moveout in particular is important for targets below the diving wave zone sampled by reflected energy alone.

Dataset and Methodology

The AWI and FWI velocity optimisation is run on the raw shot gathers from a 3D narrow-azimuth towed-streamer survey. Each shot gather consists of 14 cables of 8 km length with a 7m source tow depth. The target lies beneath the continental slope and the water bottom depth increases from left to right along the inline direction. The anisotropic starting model is derived from conventional processing.

At each bandwidth, the 5 AWI iterations are followed by 5 FWI iterations with each iteration using 20% of the shots. The forward modelling imposes Gardner's law for density. All free-surface effects are retained and no pre-processing is applied to the traces beyond bandpass filtering for progressively widening the frequency range through blocks of iterations.

Iteration block frequencies are progressively increased from 4 Hz to 18 Hz in 8 stages with interleaved AWI and FWI and then from 10 Hz to 18 Hz in 4 stages with FWI alone. These are roll-off frequencies with the shaped data at each iteration having bandwidth up to 20 Hz. In all this totals as 100 iterations, 20 passes through the shots, 8 with the AWI and 12 with the FWI cost functions.

The run was conducted using computation hardware provisioned from Amazon Web Services on the Spot market. The on-demand nature of cloud compute facilitated rapid experimentation of optimisation parameters, allowing us to quickly test the efficacy of AWI for this particular inversion. Using common node types, we were able to compute all wavefields (minimum of 3) required for a shot over its computational domain within an average of 30 minutes wall-time. This scales to having each compute node responsible for just 1 or 2 shots per iteration (using 400-800 nodes) and thus we

were able to assess whether a particular inversion strategy is effective within a few hours, without having to queue for resources on a shared cluster environment.

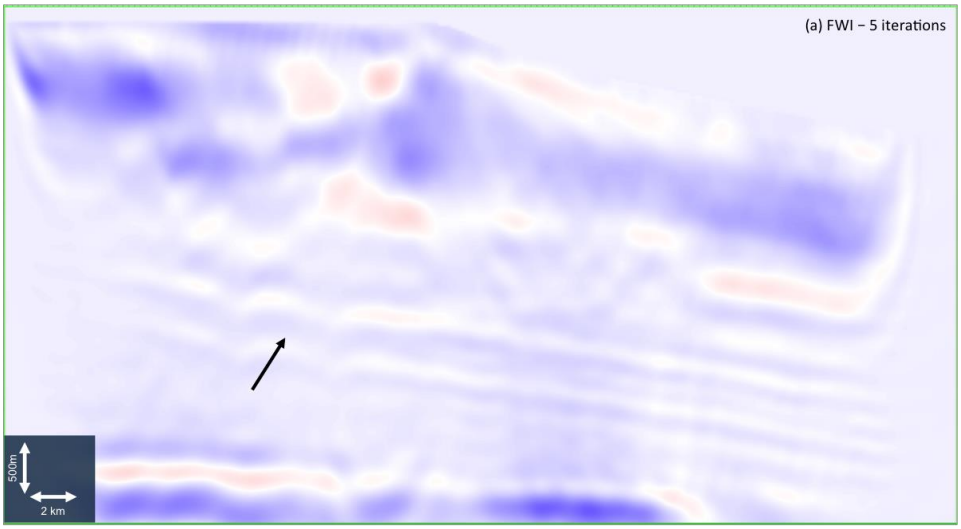

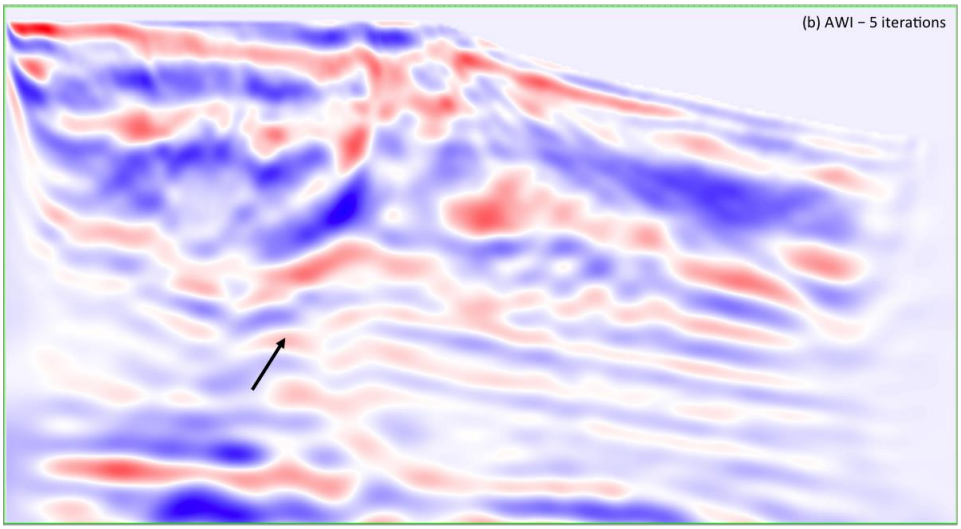

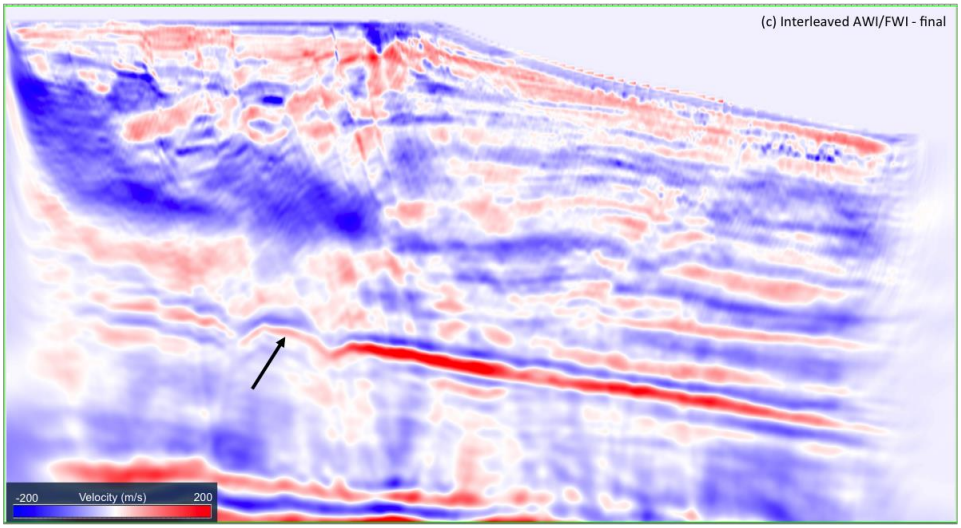

Figure 1 *Model update relative to the starting model of (a) FWI – 5 iterations, (b) AWI – 5 iterations and (c) interleaved AWI/FWI – 100 iterations. This confirms the need for AWI to penetrate deep enough to resolve the target.*

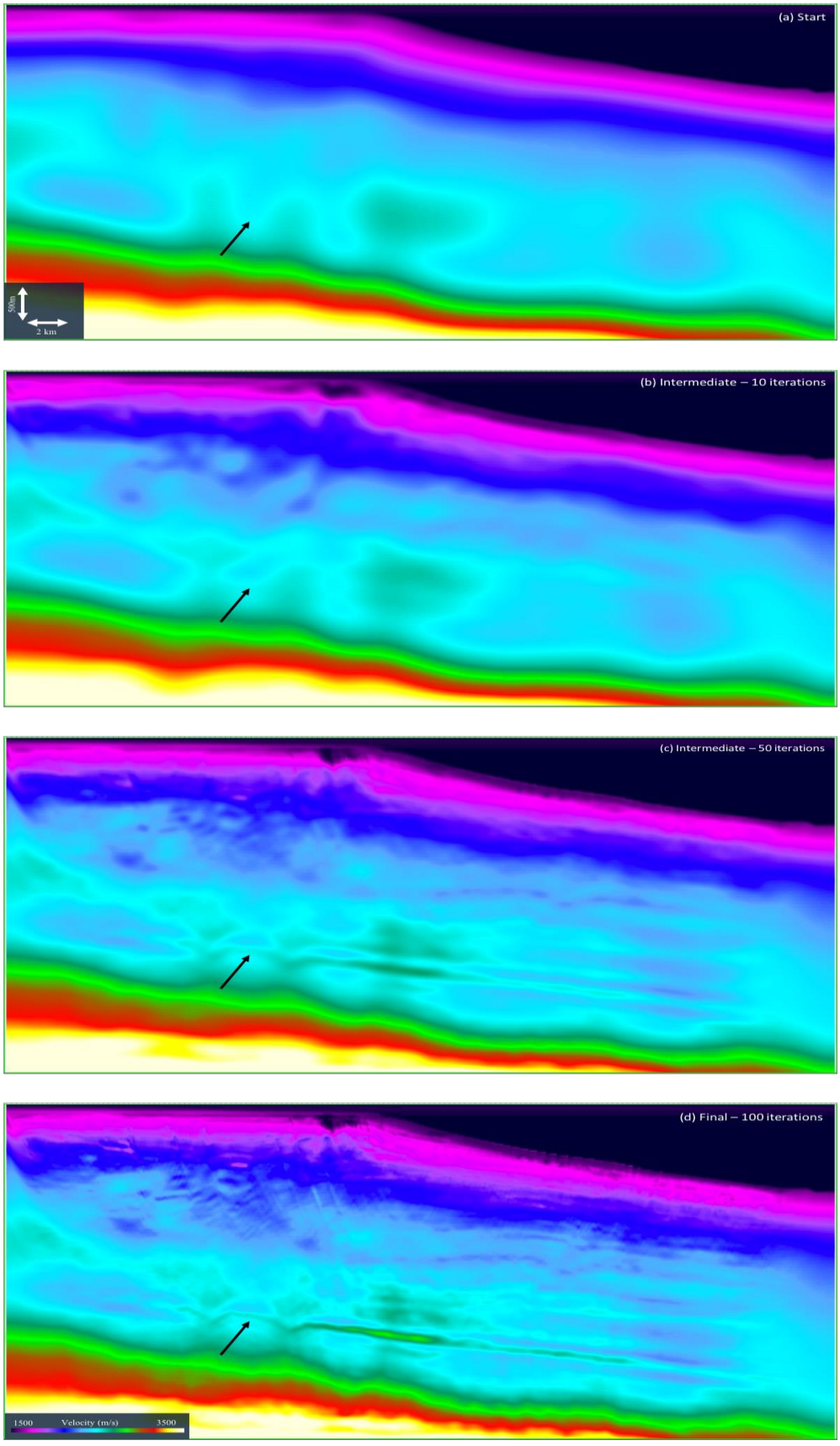

Figure 2 *Model evolution of interleaved AWI/FWI from (a) starting to (d) final model showing the broadband reconstruction of the target below 3km.*

Results

Initially we compared the effect of running 5 iterations of AWI to 5 iterations of FWI. The update relative to the starting model in both cases is shown in Figure 1. This demonstrated the superior update of AWI in particular the dominance over FWI in recovering velocity contrasts at target depths.

Then we ran the 100 iterations of AWI and FWI in interleaved fashion with the model evolution shown in Figure 2. This systematically updated the macro model giving a broadband reconstruction within and below the diving wave zone. The target highlighted by the arrow focussed with iteration and no multiple contamination was evident in the result.

The ultimate test of global minimum convergence for the velocity optimisation was the full-wavefield alignment of predicted and observed data. In Figure 3, we see the predicted data generated by the updated velocity models. The pre-critical reflections get accurately reconstructed and the post-critical reflections and diving waves align with the field data to give a high degree of data match.

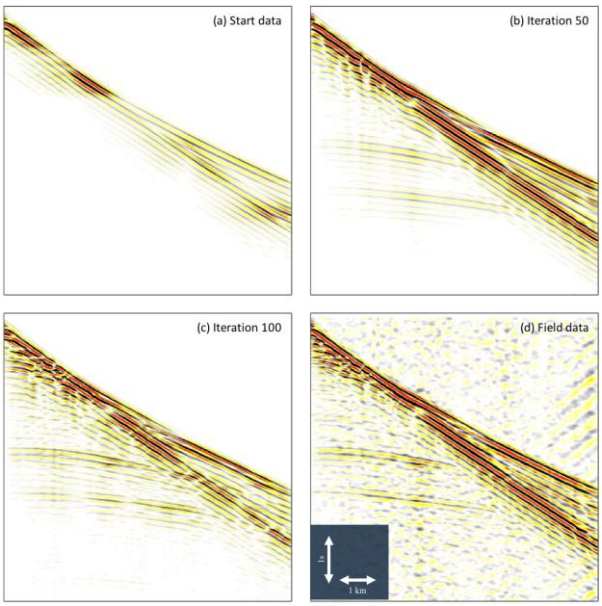

Figure 3 *Modelled shots from (a) starting model, (b) iteration 50, (c) iteration 100 with successively increased fit with (d) field data. The inversion is being driven by the refractions and the reflections.*

Conclusion

The advantages interleaving AWI and FWI are clearly demonstrated here. The inversion scheme which proceeds from low to high frequencies gives long to short wavelength updates below the reach of diving waves for building the macro model down to target depths.

Due to the insensitivity of AWI to cycle-skipping, the scheme can be applied an early stage in the model building sequence without waiting for the velocity model to increase in accuracy. This makes it a fully data-driven wave-equation based alternative to the commonly used approach of interleaving tomography with FWI for high-resolution velocity-model building.

References

Tarantola, A., 1984, Inversion of seismic reflection data in the acoustic approximation: Geophysics, 49, 1259–1266.

Warner, M. and Guasch, L. [2016] Adaptive waveform inversion: Theory. *Geophysics*, **81**(6), R429-R445.